

Heating asymmetry induced by tunneling current flow in magnetic tunnel junctions

E. Gapihan, J. Hérault, R. C. Sousa, Y. Dahmane, B. Dieny, L. Vila, I. L. Prejbeanu, C. Ducruet, C. Portemont, K. Mackay, et al.

► To cite this version:

E. Gapihan, J. Hérault, R. C. Sousa, Y. Dahmane, B. Dieny, et al.. Heating asymmetry induced by tunneling current flow in magnetic tunnel junctions. Applied Physics Letters, American Institute of Physics, 2012, 100, pp.202410. 10.1063/1.4719663 . cea-00853157

HAL Id: cea-00853157

<https://hal-cea.archives-ouvertes.fr/cea-00853157>

Submitted on 1 Jul 2020

HAL is a multi-disciplinary open access archive for the deposit and dissemination of scientific research documents, whether they are published or not. The documents may come from teaching and research institutions in France or abroad, or from public or private research centers.

L'archive ouverte pluridisciplinaire **HAL**, est destinée au dépôt et à la diffusion de documents scientifiques de niveau recherche, publiés ou non, émanant des établissements d'enseignement et de recherche français ou étrangers, des laboratoires publics ou privés.

Heating asymmetry induced by tunneling current flow in magnetic tunnel junctions

Cite as: Appl. Phys. Lett. **100**, 202410 (2012); <https://doi.org/10.1063/1.4719663>

Submitted: 09 October 2011 . Accepted: 04 May 2012 . Published Online: 18 May 2012

E. Gapihan, J. Hérault, R. C. Sousa, Y. Dahmane, B. Dieny, L. Vila, I. L. Prejbeanu, C. Ducruet, C. Portemont, K. Mackay, and J. P. Nozières



View Online



Export Citation

ARTICLES YOU MAY BE INTERESTED IN

[Spin torque switching of perpendicular Ta|CoFeB|MgO-based magnetic tunnel junctions](#)
Applied Physics Letters **98**, 022501 (2011); <https://doi.org/10.1063/1.3536482>

[Increase of temperature due to Joule heating during current-induced magnetization switching of an MgO-based magnetic tunnel junction](#)
Applied Physics Letters **92**, 233502 (2008); <https://doi.org/10.1063/1.2943151>

[Tunneling hot spots and heating in magnetic tunnel junctions](#)
Journal of Applied Physics **95**, 6783 (2004); <https://doi.org/10.1063/1.1667413>

Lock-in Amplifiers
up to 600 MHz



Heating asymmetry induced by tunneling current flow in magnetic tunnel junctions

E. Gapihan,¹ J. Hérault,¹ R. C. Sousa,¹ Y. Dahmane,¹ B. Dieny,¹ L. Vila,² I. L. Prejbeanu,³ C. Ducruet,³ C. Portemont,³ K. Mackay,³ and J. P. Nozières³

¹SPINTEC, URA 2512 CEA/INAC-CNRS, Grenoble, France

²SP2M/NM, CEA/INAC, Grenoble, France

³Crocus Technology, 4 Place Robert Schuman 38025 Grenoble, France

(Received 9 October 2011; accepted 4 May 2012; published online 18 May 2012)

In this work, exchange bias was used as a probe to characterise the temperature profile induced by the inelastic relaxation of electrons tunnelling across a MgO barrier. Thermally assisted magnetic random access memory (TA-MRAM) cells comprising a magnetic tunnel junction (MTJ) with a reference pinned layer and a FeMn exchange biased storage layer were used. The pinning direction of the ferromagnetic storage layer is reversed when heated above the blocking temperature of the antiferromagnetic layer (FeMn). The power density required to reach this blocking temperature in the FeMn layer depends on the current polarity, indicating that the heat source term associated with the current flowing through the barrier depends itself on the current direction in contrast to simple Joule heating. This effect is due to the mechanism of energy dissipation in tunnelling. The tunnelling itself is ballistic i.e., without dissipation. However, after tunnelling, the hot electrons very quickly relax to the Fermi energy thereby losing their excess energy in the receiving electrode. Therefore, the heat is essentially generated on one side of the barrier so that the whole profile of temperature throughout the pillar depends on the current direction. Full 3D thermal simulations also confirmed the temperature profile asymmetry. The proper choice of heating current direction (i.e., voltage polarity applied to the MTJ) can yield a reduction of about 10% in the heating power density required to enable writing in thermally assisted MRAM cells. © 2012 American Institute of Physics. [<http://dx.doi.org/10.1063/1.4719663>]

Magnetic random access memories (MRAMs) based on magnetic tunnel junctions (MTJs) have been developed according to different write concepts. In thermally assisted MRAM (TA-MRAM), write selectivity is achieved by using an exchange biased storage layer and applying a magnetic field while a current through the cell heats the antiferromagnet (AF) of the storage layer above its blocking temperature, typically above 150°C.¹ The magnetization of the storage layer is set by the applied field and frozen in the new direction upon cooling below the blocking temperature of the AF layer. An alternative write scheme uses spin transfer torque (STT) to reverse the storage layer direction without the need of an applied magnetic field. The STT approach can also be used together with an AF pinned storage layer, effectively combining STT writing with the improved data retention offered by a pinned storage layer. It is therefore important to characterize and understand the heating process of the tunnel junction and in particular the temperature increase at the storage layer AF as a function of the current polarity. This is, in particular, important for the thermally assisted STT write concept requiring current to flow in opposite directions to set the parallel or anti-parallel (AP) configurations. In this letter, the antiferromagnet of the pinned storage layer in a TA-MRAM cell was used to probe the temperature increase depending on the current flow direction. An asymmetry in the temperature increase related to the mechanism of energy dissipation in MTJ is observed for the first time.

The study was carried out on TA-MRAM cells² based on MTJs of composition buffer layer/PtMn 20/CoFe 2/Ru 0.74/CoFeB 2/Mg 1.1 plasma oxidized/CoFeB 1/CoFe 1/NiFe

3/FeMn 12/Ta 5 (thicknesses in nm). After the deposition, the samples were annealed at 300°C under a magnetic field of 1 T for 90 min. The storage layer exchange bias (H_{ex}) and the coercivity (H_c) were measured using a vibrating sample magnetometer (VSM) prior to nano-fabrication. The pinned storage layer showed an exchange bias of 220 Oe at the wafer level and a coercive field of 35 Oe. The quasi-static blocking temperature of the 12 nm thick FeMn antiferromagnet was measured to be 170°C. This was obtained from quasi-static magnetoresistance measurements of similar spin-valve type structures with identical FeMn layers.

The junctions were defined by advanced photo lithography and patterned to their final area dimensions first by reactive ion etching of a hard mask followed by ion-beam etching of the magnetic stack.³ During the ion-beam etch step, wafers were etched with a 40° angle and 20 rpm rotation. The final dimension of the fabricated circular pillars was 0.2 μm diameter. Quasi-static electrical measurements show a maximum TMR signal of 140% and a resistance-area product ($R \times A$) of 32 Ω μm².

The experimental setup consisted of an Agilent 81103 A pulse generator and a Veeco QSW magnetoresistance probe system. This setup was used to measure the magnetoresistance loop and to apply the heating voltage pulses. To write a TA-MRAM bit, a heating voltage pulse was applied under a 300 Oe magnetic field to ensure magnetic saturation. The width of the heating voltage pulse was 50 ns. The field was continuously applied during the heating phase as well as during the cooling to properly set the new desired pinning direction of the storage layer. After each heating pulse, once the

cell has cooled down to the standby temperature (i.e., typically 15 ns after the end of the heating pulse), the pinned storage layer exchange bias was recorded as a function of the heating pulse voltage amplitude, polarity, and width.

Before each heating pulse test, a first initialization step was used to set the storage layer in the same initial state. This initial reset pulse had a power density of $28 \text{ mW } \mu\text{m}^{-2}$ (0.95 V) and was applied under a -300 Oe field. The hysteresis loop measured after this reset step shows a positive exchange bias field of 140 Oe as shown in Fig. 1, setting the initial magnetization configuration in the AP configuration corresponding to the high resistance state. The hysteresis loop after applying a 50 ns pulse with a power density of $15 \text{ mW } \mu\text{m}^{-2}$ (0.7 V) is shown as an example of a fully reversed storage layer. The loop is now shifted towards negative field indicating that the FeMn exchange bias field has been reversed so that the remanent state in zero field now corresponds to the low resistance state.

This writing procedure was repeated for different pulse widths from 10 ns to 1 ms . The resulting storage layer exchange bias for positive voltage pulse polarity, i.e., electrons tunneling from the bottom reference electrode to the top storage electrode, is shown in Fig. 2(a). The exchange bias field is consistently reversed from $+140 \text{ Oe}$ to -140 Oe . The heating power density required for writing increases as the pulse width is decreased since the blocking temperature increases for shorter heating times.⁴ For 50 ns pulses, H_{ex} saturates at above $15 \text{ mW } \mu\text{m}^{-2}$. In these measurements, each data point corresponds to an average of 40 measurements.

Figure 2(b) shows the data for negative voltage pulse polarity, i.e., electrons flowing from the top to the bottom electrode, with the same general trend but nevertheless some quantitative differences. The point where H_{ex} crosses the zero field line is plotted for positive and negative polarity in Fig. 3. This clearly shows a reduction of the required write power density throughout all time ranges. When the electrons tunnel into the top FeMn pinned storage layer, there is a reduction in the write power density of about $2 \text{ mW } \mu\text{m}^{-2}$. This can be explained as follows: the tunneling of electrons is a ballistic event during which the electrons keep their energy. Therefore, if a bias voltage V is applied across the

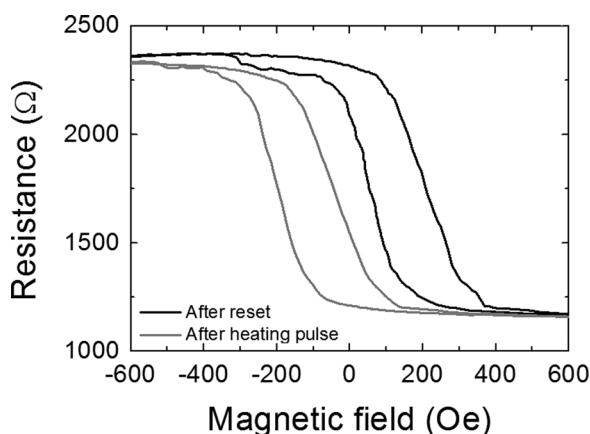


FIG. 1. Minor hysteresis loops associated with the storage layer before and after application of 50 ns pulses of $50 \text{ mW } \mu\text{m}^{-2}$ under a magnetic field of $\pm 300 \text{ Oe}$.

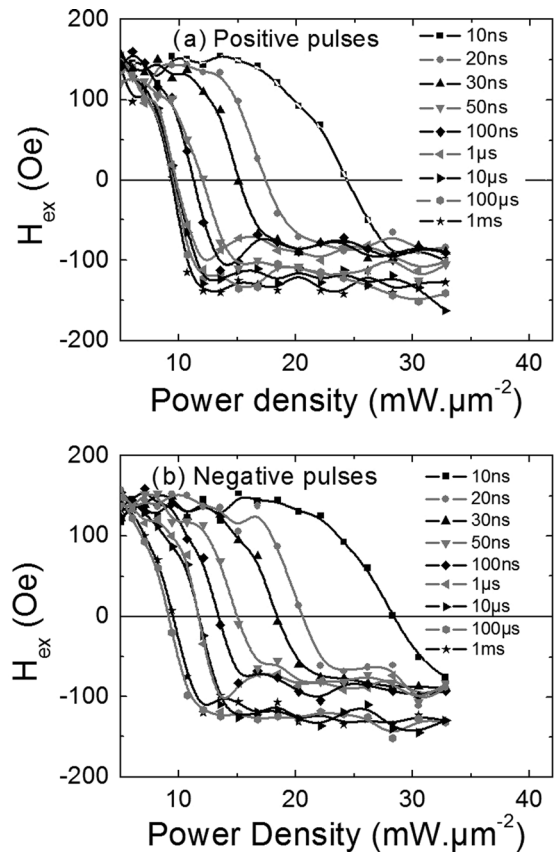


FIG. 2. Reversal of the exchange bias field of the storage layer magnetization by applying heating pulses of various power and duration from 10 ns up to 1 ms under $+300 \text{ Oe}$. (a) Voltage pulse of positive polarity was used i.e., electrons tunneling from reference layer to storage layer. Between each experiment, the magnetization of the storage layer is reset in a -300 Oe field (inducing a positive exchange bias) and written in a $+300 \text{ Oe}$ field (inducing a negative exchange bias). (b) Voltage pulse of negative polarity was used i.e., electrons tunneling from storage layer to reference layer. As before, between each experiment, the magnetization of the storage layer is reset in a -300 Oe field and written in a $+300 \text{ Oe}$ field.

tunneling barrier, the electrons are injected as hot electrons in the receiving electrode. In this electrode, they quickly relax to the Fermi energy by inelastic scattering within a length scale given by the inelastic mean free path typically of the order of 1 nm in CoFe alloys. In the emitting electrode, some heat can also be produced due to the fact that under a

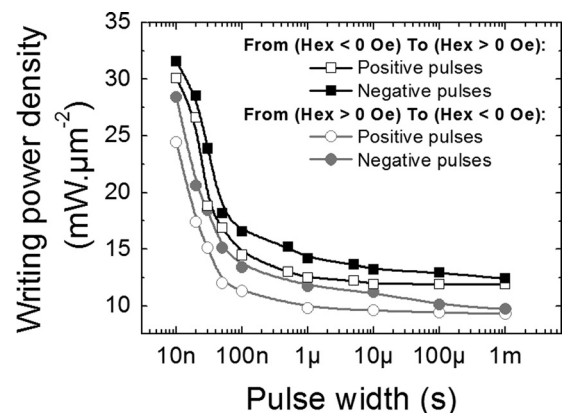


FIG. 3. Write power density required to write the storage layer versus heating pulse duration from 10 ns to 1 ms .

bias V , electrons within a band from the Fermi energy ε_F to $\varepsilon_F - V$ are allowed to tunnel. Some inelastic relaxation therefore may also take place since the states below ε_F which have been emptied by tunneling electrons must be refilled. However, this heat production becomes highly asymmetric when the bias voltage increases since the probability of tunneling varies exponentially as a function of the barrier height seen by each electron implying that mostly electrons from ε_F do tunnel through the barrier. As a result of this heating asymmetry, for the same power density, this results in a higher temperature rise in the receiving electrode. This higher temperature then propagates to the adjacent layers through usual heat diffusion. Data show that this effect is quite significant since the same temperature rise can be achieved in the FeMn antiferromagnet with a power density that can be reduced by 10% by applying the appropriate voltage polarity. The applied heating current densities are between 1.7 and 3.1×10^6 A/cm². The spin transfer torque effects are expected to play a minor role at these current densities in these structures because of their relatively thick storage layer. To confirm that spin transfer torque effect is not significant, the same experiments were performed with a reset condition that sets a negative exchange bias field in the storage layer, prior to each switching heating pulse. This sets the initial tunnel junction magnetization in the parallel (P) configuration, low resistance state. As shown in Fig. 3, a lower write power density continues to be observed for the positive pulse polarity (electrons tunnelling from reference layer to storage layer). This would not be the case if spin transfer torque was responsible for the observed write power density reduction. The same voltage polarity would not help the storage layer reversal both from AP to P configuration and from P to AP. This seems to exclude any spin torque related effects in the observed influence of voltage polarity/current direction. Fig. 3 nevertheless shows that the required current densities for switching from positive to negative exchange bias are lower than for switching from negative to positive exchange bias whatever the current direction. This observation may be ascribed to a positive stray field from the reference layer acting on the storage layer which would favor negative exchange bias of the storage layer.

Numerical 3D thermal simulations were performed using FEMLAB heat equation solver to further confirm the observed polarity dependent temperature asymmetry. Considering that in our experiments the applied voltage pulse amplitude was typically of 0.7 V, we assumed that all the heat was produced into the arrival electrode following an exponential decrease law. The power density was then described as

$$jV/l * \exp(-x/l),$$

where j is the current density, V is the voltage drop across the tunnel barrier, and l is the inelastic scattering mean free path in the receiving electrode. The heat diffusion equation was then solved for our specific device geometry, using the quasi static mode to obtain equilibrium temperature solution. The power density used for the simulation was 15 mW μm^{-2} , corresponding to the jV factor in the above expression. The inelastic mean free path was assumed to be 1 nm.

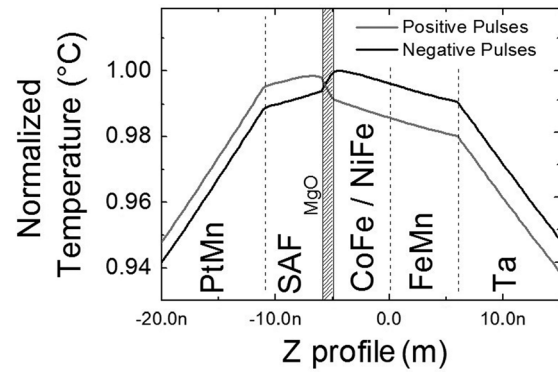


FIG. 4. Thermal simulation of the temperature profile throughout the studied structure.

For the MgO barrier, the following values of thermal conductivity k , heat capacity C_p , and density ρ were used: $k = 37$ W m^{-1} K^{-1} , $C_p = 796$ J K^{-1} kg^{-1} , and $\rho = 390$ kg m^{-3} . The calculation also tried to take into account the fact that heat conduction in metals relies primarily on electrons, while in insulators it is a phonon dominated process. Therefore, heat transfer across the interface requires electron-phonon heat transfer. This interfacial thermal conductance was assumed to be 1 GW m^{-2} K^{-1} .⁵

The calculated temperature profile near the MTJ MgO barrier is shown in Figure 4. Two different temperature profiles are clearly observed, depending on the current direction i.e., on which side of the barrier the heat is being generated from the electron tunnelling process. The MgO tunnel barrier also increases the temperature difference because it acts as a thin thermal barrier. Depending on the current direction, the temperature difference in the FeMn layer is about 1%, which is lower than the experimentally observed difference, underlining the need of more realistic material parameters to be used for the patterned thin film stack. In particular, this seems to indicate that the heat diffusion through the tunnel barrier is lower than presently assumed in the simulation which may be ascribed to additional interfacial thermal conductance at the MgO/magnetic metal interfaces.

This work showed that the direction of the tunneling current in magnetic tunnel junctions can have a significant influence in the final temperature profile within the MTJ. A FeMn antiferromagnet was used as a thermal sensor. The temperature rise in the vicinity of the barrier in TA-MRAM write conditions may vary by 10% depending on the voltage polarity/current direction. This is attributed to the mechanism of energy dissipation during tunnelling and particularly to the inelastic relaxation of hot electrons taking place in the receiving electrode. The conclusion was qualitatively supported by simulations. The effect can be used to increase the heating efficiency in TA-MRAM cells or to minimize the temperature increase of the storage layer while reading cell data. In addition, in the context of spin-caloritronics, this effect can be used to temporarily generate extremely strong temperature gradient across a tunnel barrier giving rise to interesting thermoelectric effect⁶ accompanying the cooling of the cell or magnetization switching induced by spin current resulting from the temperature gradient.

This work was supported in part by the French National Research Agency under the ANR-07-NANO-052-02 Project as well as the ERC Adv Grant HYMAGINE 246942.

¹I. L. Prejbeanu, M. Kerekes, R. C. Sousa, H. Sibuet, O. Redon, B. Dieny, and J. P. Nozieres, *J. Phys.: Condens. Matter* **19**, 165218 (2007).

²E. Gapihan, R. C. Sousa, J. Hérault, C. Papisoi, M. T. Delaye, B. Dieny, I. L. Prejbeanu, C. Ducruet, C. Portemont, K. Mackay *et al.*, *IEEE Trans. Magn.* **46**(6), 2486–2488 (2010).

³K. Sugiura, S. Takahashi, M. Amano, T. Kajiyama, M. Iwayama, Y. Asao, N. Shimomura, T. Kishi, S. Ikegawa, H. Yoda *et al.*, *Jpn. J. Appl. Phys. Part 1* **48**, 08HD02 (2009).

⁴C. Papisoi, R. Sousa, J. Herault, I. L. Prejbeanu, and B. Dieny, *New J. Phys.* **10**, 103006 (2008).

⁵A. Majumdar and P. Reddy, *Appl. Phys. Lett.* **84**(23), 4768 (2004).

⁶W. Lin, M. Hehn, L. Chaput, B. Negulescu, S. Andrieu, F. Montaigne, and S. Mangin, *Nat. Commun.* **3**, 744 (2012).